

THE EVOLUTION OF A CRYSTAL SURFACE: ANALYSIS OF A 1D STEP TRAIN CONNECTING TWO FACETS IN THE ADL REGIME

HALA AL HAJJ SHEHADEH, ROBERT V. KOHN, AND JONATHAN WEARE

ABSTRACT. We study the evolution of a monotone step train separating two facets of a crystal surface. The model is one-dimensional and we consider only the attachment-detachment-limited regime. Starting with the well-known ODE's for the velocities of the steps, we consider the system of ODE's giving the evolution of the "discrete slopes." It is the l^2 -steepest-descent of a certain functional. Using this structure, we prove that the solution exists for all time and is asymptotically self-similar. We also discuss the continuum limit of the discrete self-similar solution, characterizing it variationally, identifying its regularity, and discussing its qualitative behavior. Our approach suggests a PDE for the slope as a function of height and time in the continuum setting. However existence, uniqueness, and asymptotic self-similarity remain open for the continuum version of the problem.

1. INTRODUCTION

The surface of a crystal below the roughening temperature consists of steps and terraces. Atoms detach from the steps, diffuse across terraces, and reattach at new locations, inducing an overall evolution of the crystal surface, see e.g. [2, 11, 18]. It is important to study this evolution, because the manufacture of crystal films lies at the heart of modern nanotechnology.

Our present understanding is surprisingly incomplete. Asymptotically self-similar behavior has been observed numerically in a variety of one-dimensional and radial settings [6, 7, 8, 9, 10, 13, 17], but has rarely been explained. The continuum limit of step evolution has received considerable attention, see e.g. the references just cited and also [3, 5, 14, 16, 19, 20, 24, 25, 26], but the correct treatment of the free boundary condition at the edge of a facet remains unclear. Many authors have suggested using a Mullins-style thermodynamic approach, see e.g. [12, 21, 22, 23], however there is evidence in the radial setting that this is not consistent with the continuum limit of step motion [13].

This paper explores the step dynamics and its continuum limit in what is perhaps the simplest possible setting: a monotone one-dimensional step train connecting two unbounded facets (see Figure 1) in the attachment-detachment-limited (ADL) regime. (The physics underlying our model, including the meaning of being attachment-detachment-limited, are explained in Appendix A.) Our main accomplishments include:

Date: October 12, 2010.

Key words and phrases. steepest descent, self similar solution, facet, epitaxial relaxation.

Please address all correspondences to Hala Al Hajj Shedaheh.

This research was partially supported by NSF through grant DMS-0807347. JW was supported in part by the Applied Mathematical Sciences Program of the U.S. Department of Energy under Contract DEFG0200ER25053.

- (a) identification of a natural steepest-descent structure;
- (b) a proof that the evolution is asymptotically self-similar as $t \rightarrow \infty$ with the number of steps N held fixed; and
- (c) a detailed analysis of the continuum self-similar solution (the limit of the discrete self-similar solutions as $N \rightarrow \infty$).

As noted above, many authors have observed self-similar behavior in step-based models. To the best of our knowledge, however, we are the first to provide a systematic, mathematically rigorous explanation. Our viewpoint suggests a PDE for the evolution of the slope profile in the continuum limit, but we do not prove asymptotic self-similarity in the continuum setting.

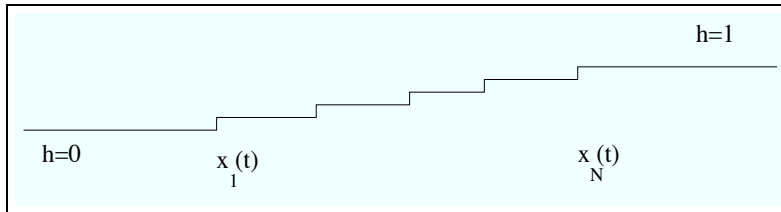


FIGURE 1. Step train connecting two unbounded facets.

Most of the literature on PDE-based models of crystal surfaces focuses on the height as a function of space and time. Our approach is different: we focus on the slope as a function of height and time. This viewpoint has several key advantages:

- the steepest-descent structure mentioned above emerges from this viewpoint (combined with our choice of ADL dynamics);
- there is no free boundary at the edge of a facet, since the slope is defined on a known interval $0 < h < 1$;
- the problem with finitely many steps is a natural finite-difference approximation of a PDE.

We are not the first to focus on the slope as a function of height. Ozdemir and Zangwill used this viewpoint to great advantage in [17], and our slope PDE (2.9) is precisely the specialization of their equation (32) to the ADL setting. Their numerical observations included the existence and stability of a self-similar solution. Our results complement theirs, by providing (among other things) a new variational characterization of the self-similar solution and a rigorous proof of its stability. Other recent papers with a viewpoint similar to ours (focusing on slope as a function of height) include [5, 6].

PDE methods guide much of our analysis, even in the discrete setting. For example, the fact that the steps neither collide nor go to infinity in finite time is proved using a simple “energy identity.” Our proof of self-similarity uses a dynamical-systems-type viewpoint that has been applied to many PDE’s [1, 4]. Indeed, we show that the evolution “in similarity variables” has a steepest-descent character, and the associated “energy” is convex. The self-similar solution is its global minimizer, and the resulting variational characterization provides additional information about its qualitative properties.

Our analysis is restricted to the ADL regime, where the slope evolution has a convenient steepest-descent structure. The recent paper [15] is closely related but complementary: it considers a variety of different physical models (not just ADL), but limits its attention to the self-similar solutions (not

addressing their stability). By taking the continuum limit $N \rightarrow \infty$, [15] identifies the behavior of the self-similar solution near the boundary $h = 0, 1$. In the ADL setting its results are entirely consistent with ours, though its method is entirely different.

The rest of this Introduction gives a brief overview of our viewpoint, methods, and main achievements. We start in Section 2 by reviewing the step motion law. Then we show (following the lead of [17]) that the ODE describing the evolution of the discrete slopes $y_i = \frac{1/N}{x_{i+1} - x_i}$ is the finite-difference analogue of the PDE

$$(1.1) \quad u_t = -u^2(u^3)_{hhhh}$$

with boundary conditions $u(0, t) = u(1, t) = 0$ and $(u^3)_{hh}(0, t) = (u^3)_{hh}(1, t) = 0$. The slope evolution has a convenient steepest-descent structure in both the discrete and continuum settings. Focusing here on the continuous case: (1.1) does steepest descent for

$$E(u) = \int_0^1 \frac{1}{6} [(u^3)_{hh}]^2 dh$$

subject to $u(0) = u(1) = 0$, in precisely the same sense that the heat equation does steepest descent for the Dirichlet integral. The steepest-descent structure is used in Section 2 to prove that steps cannot collide. We also present some numerics, focusing on the qualitative properties of the step and slope evolutions in the continuum limit $N \rightarrow \infty$ and the large-time limit $t \rightarrow \infty$.

Section 3 shows that both the discrete and continuous versions of the problem have self-similar solutions, and discusses their properties. In the continuum, this amounts to looking for a solution of (1.1) of the form $u(t, h) = t^{-1/4} \phi(h)$. We give a variational characterization of the self-similar solution and apply it to prove uniqueness. In the continuum, the self-similar solution is not very smooth near the endpoints $h = 0, 1$; our results include a detailed characterization of its behavior.

Section 4 proves that the slope evolution is asymptotically self-similar as $t \rightarrow \infty$ with N held fixed. The proof relies on the steepest-descent structure of the evolution rewritten in “similarity variables,” combined with strict positivity of the slope and the uniqueness of the self-similar solution.

Section 5 analyzes the relationship between our discrete and continuous self-similar solutions. This amounts to studying the relationship between a certain continuous variational problem and its finite-difference approximation. The convergence rate is $N^{-5/6}$ rather than N^{-1} because the continuous solution is not very smooth at the endpoints.

We close, in Section 6, with a brief discussion why rigorous analysis of the continuous slope evolution problem seems to require additional ideas. This section also discusses the apparent limitations of our slope-oriented, steepest-descent-based viewpoint.

The paper ends with two Appendices. Appendix A reviews the physics behind the step motion law. Appendix B discusses the relationship between our slope-based viewpoint and the more widely-used approach in which the surface height $h(x, t)$ solves a PDE with respect to position and time.

Acknowledgement. We thank John Ball for the observation that the energy in similarity variables is convex when viewed as a function of $v = w^3$.

2. THE DISCRETE EVOLUTION AND THE ASSOCIATED PDE

This section presents the step and slope ODE's, explaining the crucial steepest-descent structure of the slope ODE's and using it to prove global-in-time existence. We also discuss the relation between the slope ODE's and the conjectured continuum limit. The section closes with a discussion of the qualitative behavior of the step and slope equations, focusing on the behavior as $N \rightarrow \infty$ or $t \rightarrow \infty$.

2.1. Step and slope ODEs. We are interested in the evolution of a monotone one-dimensional step train in the attachment-detachment-limited regime. The ODE's for the step velocities are well-known (see e.g. [6, 7, 10, 17]). Briefly: adopting the viewpoint originated by Burton, Cabrera, and Frank [2], one finds the concentration of adatoms on each terrace, and the net flux of adatoms at each step; this determines the step velocity, by conservation of mass. The full derivation is given for the reader's convenience in Appendix A. The upshot is this: let $x_1(t) < x_2(t) < \dots < x_N(t)$ be the positions of N steps (each of height $h = 1/N$) separating our two facets (at heights $h = 0$ and $h = 1$ respectively, see Figure 1). Then the "interior" steps evolve by

$$(2.1) \quad \dot{x}_i = \mu_{i+1} - 2\mu_i + \mu_{i-1}, \quad 2 \leq i \leq N - 2$$

where μ_i (the "chemical potential") is the first variation of the step interaction energy

$$(2.2) \quad \mathcal{E} = \frac{1}{2} \sum_{i=1}^{N-1} \frac{1}{(x_{i+1} - x_i)^2},$$

with respect to x_i . Doing the differentiation, we have:

$$(2.3) \quad \mu_i = \frac{\partial \mathcal{E}}{\partial x_i} = \begin{cases} (x_2 - x_1)^{-3} & \text{when } i = 1 \\ (x_{i+1} - x_i)^{-3} - (x_i - x_{i-1})^{-3} & \text{when } 2 \leq i \leq N - 2 \\ -(x_N - x_{N-1})^{-3} & \text{when } i = N. \end{cases}$$

The evolution laws for extreme steps x_1 and x_N are different, because each has a facet on one side and a terrace on the other; their velocities are

$$(2.4) \quad \dot{x}_1 = \mu_2 - \mu_1, \quad \dot{x}_N = -\mu_N + \mu_{N-1}.$$

It will be convenient to focus not on the step positions, but rather on the "discrete slopes" defined by

$$(2.5) \quad y_i(t) = \frac{1/N}{x_{i+1}(t) - x_i(t)}, \quad 1 \leq i \leq N - 1.$$

Clearly the step ODE's imply an evolution law for the slopes. Away from the extremes, a straightforward calculation gives

$$\dot{y}_i = -y_i^2 \Delta_i \Delta y^3 \quad \text{for } i = 3, \dots, N - 3$$

where $\Delta \xi$ is the second-order finite difference of $\xi = (\xi_1, \dots, \xi_{N-1})$ with respect to height:

$$(2.6) \quad \Delta_i \xi = N^2 (\xi_{i+1} - 2\xi_i + \xi_{i-1}).$$

At the extremes, the analogous calculation gives

$$\begin{aligned}\dot{y}_1 &= -y_1^2 N^2 [\Delta_2 y^3 - 2N^2 (y_2^3 - 2y_1^3)] \\ \dot{y}_2 &= -y_2^2 N^2 [\Delta_3 y^3 - 2\Delta_2 y^3 + N^2 (y_2^3 - 2y_1^3)] \\ \dot{y}_{N-2} &= -y_{N-2}^2 N^2 [N^2 (-2y_{N-1}^3 + y_{N-2}^3) - 2\Delta_{N-2} y^3 + \Delta_{N-3} y^3] \\ \dot{y}_{N-1} &= -y_{N-1}^2 N^2 [-2N^2 (-2y_{N-1}^3 + y_{N-2}^3) + \Delta_{N-2} y^3].\end{aligned}$$

This can be written much more elegantly by introducing the conventions

$$(2.7) \quad y_0 = y_N = 0 \quad \text{and} \quad \Delta_0 y^3 = \Delta_N y^3 = 0,$$

so that $\Delta_1 y^3 = N^2 (y_2^3 - 2y_1^3)$ and $\Delta_{N-1} y^3 = N^2 (-2y_{N-1}^3 + y_{N-2}^3)$ (using the first convention), and $\Delta_1 \Delta y^3 = N^2 (\Delta_2 y^3 - 2\Delta_1 y^3)$ and $\Delta_{N-1} \Delta y^3 = N^2 (-2\Delta_{N-1} y^3 + \Delta_{N-2} y^3)$ (using the second convention). With these conventions, the evolution law for the slopes becomes

$$(2.8) \quad \dot{y}_i = -y_i^2 \Delta_i \Delta y^3 \quad \text{for } i = 1, 2, \dots, N-1.$$

Since Δ is the finite-difference Laplacian with respect to height, it is natural to guess that as $N \rightarrow \infty$, our discrete slopes should be converging to a function $u(h, t)$ defined on $0 \leq h \leq 1$ such that

$$(2.9) \quad u_t = -u^2 (u^3)_{hhhh}$$

with boundary conditions $u(0, t) = u(1, t) = 0$ and $(u^3)_{hh}(0, t) = (u^3)_{hh}(1, t) = 0$. Our results are consistent with this conjecture, though they fall short of proving it.

Since the step and slope ODE's are highly nonlinear, it is not immediately obvious that they have a global-in-time solution. The main issue is whether steps can collide. We will rule out collisions and prove global-in-time existence in Section 2.3.

2.2. Steepest-descent structure. The slope ODE's (2.8) and their continuum analogue (2.9) have a natural gradient-flow structure, which is crucial to our analysis. To explain, we focus first on the ODE's, and we begin by recalling the definition of an l^2 steepest-descent.

Definition. If a and b are vectors in \mathbb{R}^d , their l^2 -inner product is given by $\langle a, b \rangle_{l^2} = \sum_{i=1}^d a_i b_i$. For any function $E : \mathbb{R}^d \rightarrow \mathbb{R}$, its l^2 -gradient (denoted by $\partial_{l^2} E$) is the vector-valued function such that $\dot{E}(a) = \langle \partial_{l^2} E(a), \dot{a} \rangle_{l^2}$ for any curve $a(t)$. The ODE $\dot{a} = f(a)$ is the l^2 -steepest descent of E when $f(a) = -\partial_{l^2} E(a)$.

Since the slope ODE's are the finite-difference version of a PDE, their analysis involves the finite-difference analogue of integration by parts. If $\xi = (\xi_1, \dots, \xi_{N-1})$, we use the standard forward and backward difference operators

$$D_i^+ \xi = N(\xi_{i+1} - \xi_i), \quad D_i^- \xi = N(\xi_i - \xi_{i-1})$$

and the second-difference operator

$$\Delta_i \xi = N^2 (\xi_{i+1} - 2\xi_i + \xi_{i-1})$$

(recall that the index indicates height, and the height increment is $1/N$). Note that $D_i^- D^+ \xi = D_i^+ D^- \xi = \Delta_i \xi$, and $D_i^+ D^+ \xi = \Delta_{i+1} \xi$. The analogue of integration by parts is summation by parts:

$$\sum_{k=m}^n f_k D_k^+ g = - \sum_{k=m}^{n+1} g_k D_k^- f + N f_{n+1} g_{n+1} - N f_{m-1} g_m$$

which is equivalent to

$$(2.10) \quad \sum_{k=m}^n f_k D_k^+ g = - \sum_{k=m}^n g_{k+1} D_k^+ f + N f_{n+1} g_{n+1} - N f_m g_m.$$

When ξ_0 and ξ_N are not otherwise defined we take them to be 0, so that $\Delta_1 \xi$ and $\Delta_{N-1} \xi$ are well-defined.

Proposition 2.1. *The slope ODE's (2.8) are the l^2 -steepest descent of the discrete energy*

$$(2.11) \quad E_N(y) = \frac{1}{6} \sum_{i=1}^{N-1} (\Delta_i y^3)^2.$$

Proof. Recall our convention that $\Delta_0 y^3 = \Delta_N y^3 = 0$, so the sum in (2.11) is not changed if we include the terms associated with $i = 0$ and/or $i = N$. This will be useful for the summations by parts that follow. Consider any smooth evolution $(y_1(t), \dots, y_{N-1}(t))$ and recall the convention that $y_0 = y_N = 0$. Differentiating (2.11) gives

$$\begin{aligned} \frac{d}{dt} E_N(y) &= \sum_{i=0}^{N-1} \Delta_i y^3 \cdot \Delta_i (y^2 \dot{y}) \\ &= \sum_{i=0}^{N-1} (\Delta_i y^3) D_i^+ D^- (y^2 \dot{y}). \end{aligned}$$

Summing by parts using (2.10) gives

$$\frac{d}{dt} E_N(y) = - \sum_{i=0}^{N-1} D_i^+ (\Delta y^3) D_i^+ (y^2 \dot{y}).$$

The boundary terms $\Delta_N y^3 D_N^- (y^2 \dot{y}) - \Delta_0 y^3 D_0^- (y^2 \dot{y})$ vanish since $\Delta_0 y^3$ and $\Delta_N y^3$ are equal to zero. Summing again by parts, we have

$$\frac{d}{dt} E_N(y) = \sum_{i=0}^{N-1} D_i^+ D^+ (\Delta y^3) (y_{i+1}^2 \dot{y}_{i+1})$$

where the boundary terms $-D_N^+ \Delta y^3 y_N^2 \dot{y}_N + D_0^+ \Delta y^3 y_0^2 \dot{y}_0$ vanish again since $y_0 = y_N = 0$. It follows that

$$\begin{aligned} \frac{d}{dt} E_N(y) &= \sum_{i=0}^{N-1} (\Delta_{i+1} \Delta y^3) y_{i+1}^2 \dot{y}_{i+1} \\ &= \sum_{i=1}^{N-1} (\Delta_i \Delta y^3) y_i^2 \dot{y}_i. \end{aligned}$$

The last sum is from 1 to $N - 1$ since $y_N = 0$. The last equality says

$$\frac{d}{dt} E_N(y) = \langle y_i^2 \Delta_i \Delta y^3, \dot{y}_i \rangle_{l^2}.$$

Therefore (2.8) (with the conventions $y_0 = y_N = 0$ and $\Delta_0 y^3 = \Delta_N y^3 = 0$) can be written as

$$\dot{y} = -\partial_{l^2} E_N(y).$$

□

The PDE (2.9) has an analogous steepest-descent structure: it is the L^2 steepest-descent associated with the functional

$$(2.12) \quad E(u) = \int_0^1 \frac{1}{6} [(u^3)_{hh}]^2 dh.$$

Indeed, for any sufficiently smooth $u(h, t)$ we have

$$\begin{aligned} \dot{E}(u) &= \int_0^1 (u^3)_{hh} (u^2 \dot{u})_{hh} dh \\ &= \int_0^1 (u^3)_{hhhh} u^2 \dot{u} dh + (u^3)_{hh} (u^2 \dot{u})_h \Big|_0^1 - (u^3)_{hhh} u^2 \dot{u} \Big|_0^1 \\ (2.13) \quad &= \langle (u^3)_{hhhh} u^2, \dot{u} \rangle_{L^2} + \text{boundary terms.} \end{aligned}$$

The boundary conditions $u(0, t) = u(1, t) = 0$ and $(u^3)_{hh}(0, t) = (u^3)_{hh}(1, t) = 0$ assure that the boundary terms vanish. Thus (2.9) with these boundary conditions can be written as $u_t = -\partial_{L^2} E(u)$. (In fact, the preceding calculation reveals that if one imposes $u(0, t) = u(1, t) = 0$ as the “essential boundary condition,” then $(u^3)_{hh}(0) = (u^3)_{hh}(1) = 0$ emerges as the associated “natural boundary condition,” in the sense that it is required to make the boundary term $(u^3)_{hh} (u^2 \dot{u})_h \Big|_0^1$ vanish. See (3.13) for a more careful discussion.)

These steepest-descent structures will lie at the heart of many of our arguments. In addition, they demonstrate that the slope ODE’s (2.8) are a *natural finite difference discretization* of the slope PDE (2.9), in the sense that (i) the slope ODE’s are the l^2 -steepest descent of the discrete energy E_N , (ii) the PDE is the L^2 -steepest descent of the continuum energy E , and (iii) E_N is a finite-difference approximation of E .

The calculation leading to (2.13) was easier than the proof of Proposition 2.1, because integration by parts is easier than summation by parts. This pattern will recur throughout the paper: our arguments are usually more transparent in the continuous setting. However we will sometimes be required to work in the discrete setting to achieve our goals. (For example, in the next subsection

we will prove that $y_i(t)$ stays positive for all t and all $1 \leq i \leq N - 1$, however we do not know whether $u(h, t)$ stays positive for all $0 < h < 1$.)

It is natural to ask whether the functionals $E_N(y)$ and $E(u)$ have physical meaning. The answer is yes: they give the rate at which the step interaction energy is dissipated. Indeed, in the discrete setting the interaction energy (defined by (2.2)) is a constant times $\sum_{i=1}^{N-1} y_i^2$, so our assertion follows from

Lemma 2.2. *For any solution of the slope ODE's (2.8), the l^2 norm decreases and*

$$(2.14) \quad \frac{d}{dt} \frac{1}{2} \|y\|_{l^2}^2 = -6E_N(y).$$

Proof. The functional $E_N(y) = \frac{1}{6} \sum (\Delta_i y^3)^2$ is homogeneous of degree 6, in the sense that if $\lambda y = (\lambda y_1, \dots, \lambda y_{N-1})$ then

$$E_N(\lambda y) = \lambda^6 E_N(y).$$

Differentiating with respect to λ then evaluating the result at $\lambda = 1$ we conclude that

$$(2.15) \quad \langle y, \partial_{l^2} E_N(y) \rangle_{l^2} = 6E_N(y).$$

So for any solution of the slope ODE's, Proposition 2.1 gives

$$\frac{d}{dt} \frac{1}{2} \|y\|_{l^2}^2 = -\langle y, \partial_{l^2} E_N(y) \rangle_{l^2} = -6E_N(y)$$

as asserted. \square

The same argument applies in the continuum setting, where the step interaction energy is represented by $\int_0^1 u^2 dh$. Alternatively, we can simply integrate by parts: using the PDE and its boundary conditions (and assuming the solution is regular enough to support the integration by parts) we have

$$\frac{d}{dt} \frac{1}{2} \int_0^1 u^2 dh = \int_0^1 uu_t dh = - \int_0^1 u^3 (u^3)_{hhhh} dh = - \int_0^1 (u^3)_{hh}^2 dh = -6E(u).$$

2.3. Global-in-time existence. We are ready to prove that the step and slope ODE's have a global-in-time solution.

Theorem 2.3. *The step ODE's (2.1) have a global-in-time solution for any "monotone" initial data (i.e. any $x_1(0) < x_2(0) < \dots < x_N(0)$); in particular the steps cannot collide in finite time. Also, the slope ODE's (2.8) have a global-in-time solution for any positive initial data (i.e. any $y_1(0) > 0, \dots, y_{N-1}(0) > 0$); moreover y_i remains positive for all time and each $i = 1, \dots, N - 1$.*

Proof. The standard existence theory for ODE's tells us that the solution of the step ODE's can be continued until either (a) the evolution becomes undefined because two steps collide, or (b) a step reaches infinity in finite time. Alternative (a) cannot occur, because by Lemma 2.2 each $y_i = N^{-1}(x_{i+1} - x_i)^{-1}$ remains bounded:

$$\max_{1 \leq i \leq N-1} y_i^2(t) \leq \sum_{i=1}^{N-1} y_i^2(t) \leq \sum_{i=1}^{N-1} y_i^2(0).$$

Alternative (b) is also impossible, because \dot{x}_i is a linear combination of μ_j 's, and

$$\max_{1 \leq i \leq N} |\mu_i| \leq N^3 \max_{1 \leq i \leq N-1} y_i^3$$

2.4. Qualitative behavior and numerical evidence of self-similarity. We believe that

- (a) there is a well-defined continuum limit as $N \rightarrow \infty$;
- (b) the continuum height profile $h(x, t)$ “has finite extent” and is asymptotically self-similar;
- (c) the continuum slope as a function of height and time is also asymptotically self-similar; and
- (d) the discrete evolution with N held fixed is also asymptotically self-similar.

This subsection explains the meaning of these assertions and gives some numerical evidence. The rest of the paper presents progress toward these goals. Toward (b) and (c), we shall characterize and discuss the discrete and continuous self-similar solutions. Toward (a), we shall prove convergence of the self-similar solutions as $N \rightarrow \infty$. Assertion (d) will be proved in its entirety.

Assertions analogous to (a)-(d) have been studied for a variety of one-dimensional models like the one considered here [6, 7, 10, 17] and also in some radial settings [8, 9, 12, 13]. However these studies are largely numerical or heuristic. We are the first to prove asymptotic self-similarity, to give a variational characterization of the similarity solution, and to prove convergence of the similarity solutions as $N \rightarrow \infty$. (Alas, our analysis addresses just one of the many cases considered in the articles just cited.)

As numerical evidence of (a) we point to the smoothness of the profiles shown in Figure 2, which were obtained by solving the ODE’s with $N = 51$, using equispaced steps (constant slope 1) as the initial data. The top half of the figure shows the associated height profiles at the the initial time (solid), several intermediate times (dotted), and largest time observed (solid). Notice that the step train spreads, gradually expanding its extent and decreasing its maximum slope. The bottom half of the figure shows the slope $F = h_x$ as a function of x and t , i.e. it plots $\frac{1/N}{x_{i+1}-x_i}$ against $\frac{x_i+x_{i+1}}{2}$. (We denote the slope by F not u to avoid confusion: F is the slope as a function of position and time, while u is the slope as a function of height and time.) Again, the solid curves show the slope at the initial and largest times, and the dotted curves show some intermediate times. While the slope is initially 1, it quickly becomes smoother (approaching 0 at the ends of the step train). Eventually it becomes concave and settles into a characteristic profile.

The conjecture that the continuum profile has “finite extent” means that as $N \rightarrow \infty$ the left-most and right-most steps have finite limits $x_L(t)$ and $x_R(t)$. Thus the continuum profile consists of two facets (one with $h = 0$ to the left of x_L , the other with $h = 1$ to the right of x_R) separated by a continuous step train (a smoothly-varying height profile $h(x, t)$ defined for $x_L(t) < x < x_R(t)$). For numerical confirmation, we calculated the values of $x_N(t) - x_1(t)$ as N varies (always using constant-slope-one initial data, and keeping the time t fixed). The results are given in Table 1.

TABLE 1. Numerical evidence that the profile “has finite extent” in the continuum limit: $x_N(t) - x_1(t)$ at $t = 30$ for a surface with constant slope at $t = 0$.

N	10	100	1000	2000	3000
$x_N - x_1$	10.486	10.548	9.9787	10.956	11.317

The conjectured self-similarity of the height profile says that as $t \rightarrow \infty$,

$$h(x, t) \sim H\left(\frac{x}{t^{1/4}}\right)$$

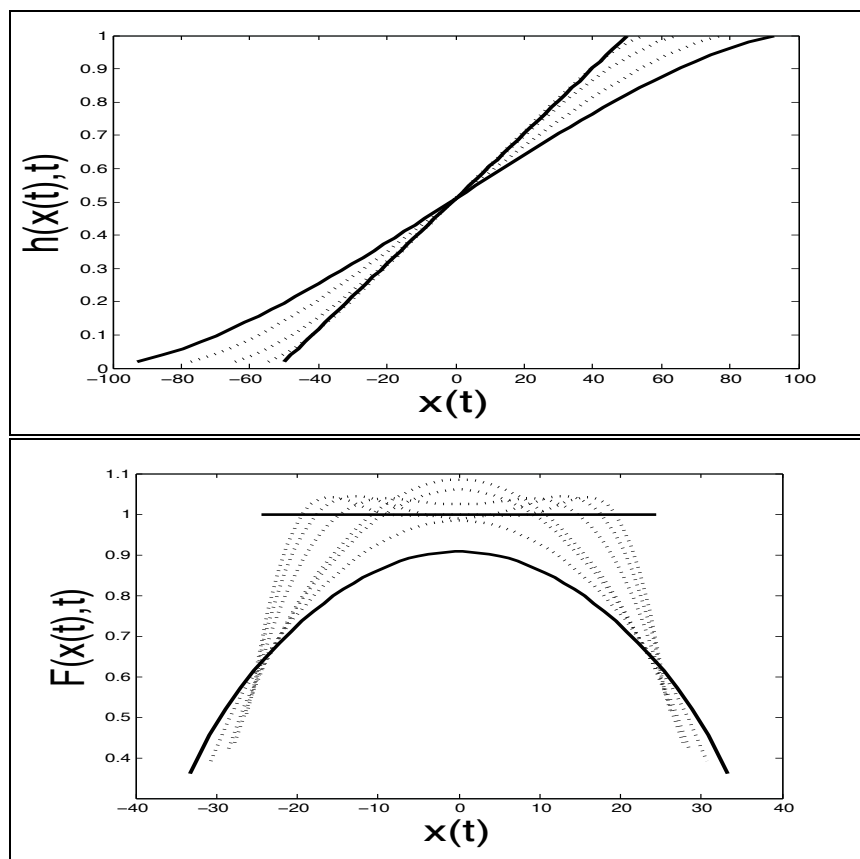


FIGURE 2. Simulation of the step equations with $N = 51$. *Top*: Surface height as a function of x at various times. *Bottom*: The discrete slope as a function of x at various times.

for some function $H(z)$. If so, then $F = h_x$ behaves as $t^{-1/4}H'(x/t^{1/4})$. Figure 3 provides numerical confirmation of such behavior, by showing that after an initial transient the profile of $t^{1/4}F$ as a function of $x/t^{1/4}$ appears to approach a limit as $t \rightarrow \infty$.

As we explained in the Introduction (and in Section 2.1), we prefer to focus on the slope ODE's rather than the step ODE's. They are more convenient due to their simple steepest-descent structure, and because the continuum limit has no free boundary. In this setting, the conjecture of asymptotic self-similarity says that as $t \rightarrow \infty$, the slope u viewed as a function of height and time satisfies

$$u(h, t) \sim t^{-1/4}\phi(h)$$

for some function ϕ defined on $[0, 1]$. Figure 4 shows the behavior of the slope ODE's (2.8) and provides graphical evidence of asymptotic self-similarity. In the top left subfigure, we plot y_i against $h_i = i/N$ starting with nonsymmetric data (the solid line). The solution quickly becomes smooth and eventually becomes symmetric and concave. The top right subfigure shows that after scaling y_i by $t^{1/4}$, the concave curves at later times collapse into a common graph (the self-similar solution).

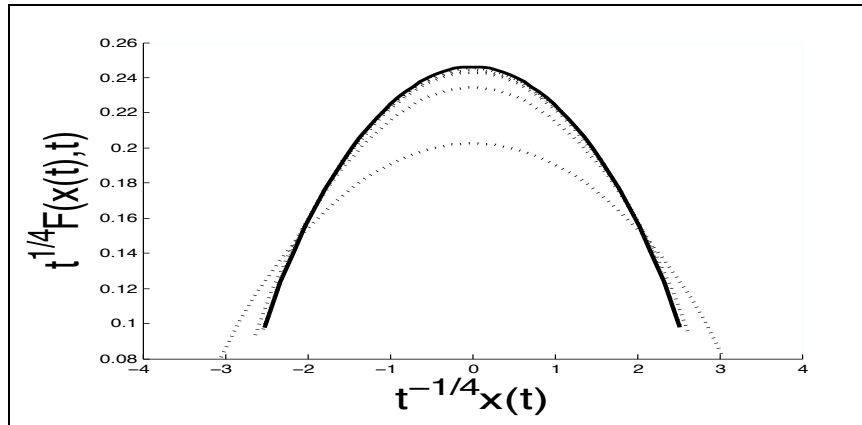


FIGURE 3. Numerical evidence of self-similarity: after scaling x by $t^{-1/4}$ and $F(x, t) = h_x(x, t)$ by $t^{1/4}$, slope profiles are asymptotically stationary.

The bottom part of Figure 4 reports the results of a similar calculation with symmetric initial data. Notice that the approach to self-similarity is much faster in the symmetric setting.

3. THE SELF-SIMILAR SOLUTION

This section discusses the similarity solution associated with the slope ODE's and their continuum analogue. Besides proving existence and uniqueness, we also obtain additional information. In particular, we show that the cube of the similarity solution is concave, and we prove (in the continuous setting) that the associated step train “has finite extent.” We shall prove asymptotic self-similarity for the discrete problem in Section 4, and we shall study the continuum limit of the similarity solutions in Section 5.

3.1. Introduction of similarity variables. We expect $t^{1/4}y_i(t)$ to become independent of t in the large-time limit. Therefore it is natural to rewrite the slope ODE's in *similarity variables*. This means making the change of variable

$$(3.1) \quad w_i(s) = (1+t)^{1/4}y_i(t), \quad s = \log(1+t).$$

One verifies that the slope ODE's (2.8) are equivalent to

$$(3.2) \quad \dot{w}_i(s) = \frac{1}{4}w_i - w_i^2 \Delta_i \Delta(w^3)$$

with the usual conventions that $w_0 = w_N = 0$ and $\Delta_0 w = \Delta_N w = 0$. Notice that $s = 0$ when $t = 0$, and $w_i(0) = y_i(0)$, so w has the same initial data as y . (This is why we scaled by $(1+t)^{1/4}$ rather than $t^{1/4}$.) The choice $s = \log(1+t)$ might seem mysterious; it has the special feature of making the evolution in similarity variables *autonomous*.

A similarity solution is a stationary solution of (3.2), i.e. vector $\phi = (\phi_1, \dots, \phi_{N-1})$ such that

$$(3.3) \quad \frac{1}{4}\phi_i = \phi_i^2 \Delta_i \Delta(\phi^3)$$

for each i , with the conventions that $\phi_0 = \phi_N = 0$ and $\Delta_0 \phi^3 = \Delta_N \phi^3 = 0$.

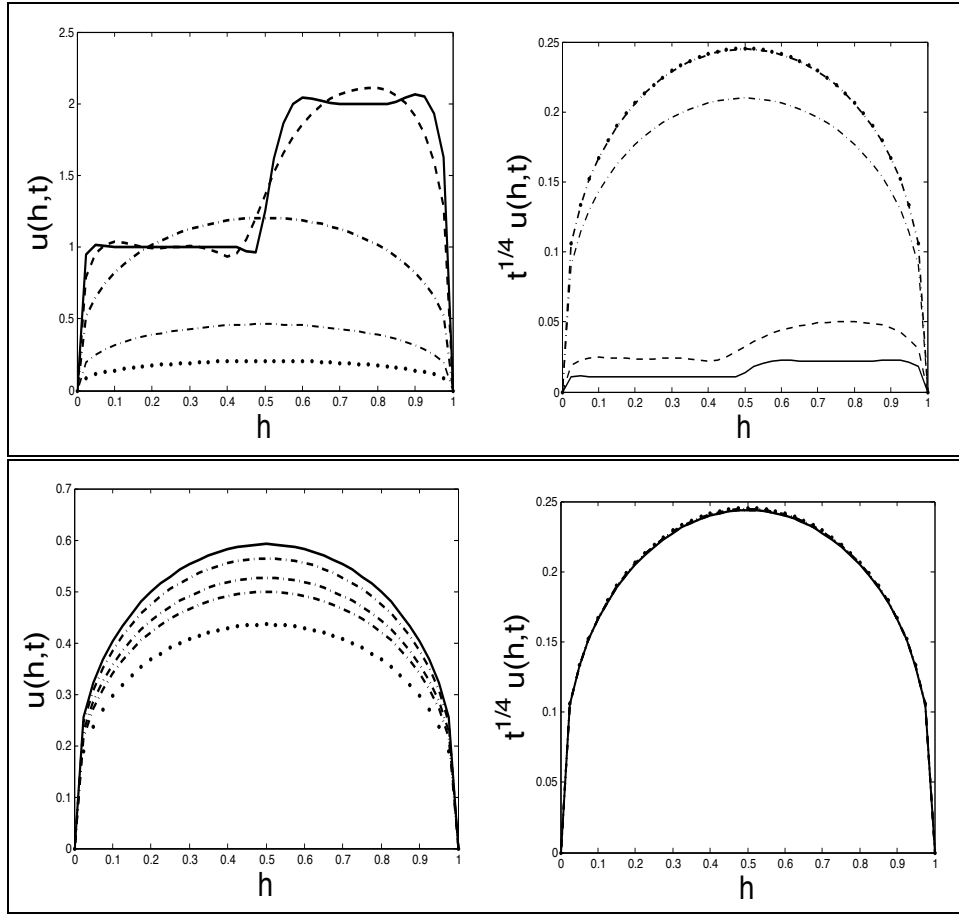


FIGURE 4. Simulation of the slope equations, with asymmetric initial data (top) and symmetric initial data (bottom). The left side shows the slope y_i as a function of height i/N at various times. The right side shows the scaled slope $t^{1/4}y_i$ as a function of height, demonstrating asymptotic self-similarity.

The introduction of similarity variables in the continuum setting is similar. One verifies that if $u(h, t)$ solves (2.9) then the function $w(h, s)$ defined by

$$(3.4) \quad w(h, s) = (1 + t)^{1/4} u(h, t), \quad s = \log(1 + t)$$

solves

$$(3.5) \quad w_s = \frac{1}{4} w - w^2 (w^3)_{hhhh}$$

with boundary conditions $w(0, t) = w(1, t) = 0$ and $(w^3)_{hh}(0, t) = (w^3)_{hh}(1, t) = 0$. A continuum similarity solution $\phi(h)$ solves the associated stationary equation

$$(3.6) \quad \frac{1}{4} \phi = \phi^2 (\phi^3)_{hhhh}$$

with $\phi(0) = \phi(1) = 0$ and $(\phi^3)_{hh}(0) = (\phi^3)_{hh}(1) = 0$.

3.2. Existence, uniqueness, and properties of the discrete self-similar solution. The evolution in similarity variables (3.2) is the l^2 steepest-descent associated with

$$(3.7) \quad SE_N(w) = \sum_{i=1}^{N-1} -\frac{1}{8}w_i^2 + \frac{1}{6}(\Delta_i w^3)^2$$

(defined using the convention that $w_0 = w_N = 0$). The proof is almost the same as that of Proposition 2.1. As a consequence, a similarity solution is simply a critical point of SE_N , and we can prove both existence and uniqueness by arguing variationally.

Theorem 3.1. *Consider the “similarity energy” $SE_N : \mathbb{R}^{N-1} \rightarrow \mathbb{R}$.*

- (a) *The minimum subject to $w_i \geq 0$ is achieved.*
- (b) *The minimizer ϕ is unique and strictly positive (i.e. $\phi_i > 0$ for $i = 1, \dots, N-1$). Moreover, it has the property that the piecewise linear graph of ϕ^3 is concave (equivalently, $\Delta_i \phi^3 \leq 0$ for $i = 1, \dots, N-1$).*
- (c) *This ϕ is the unique positive critical point of SE_N .*

Proof. It is convenient to work with $v_i = w_i^3$, in terms of which $SE_N(w)$ equals

$$(3.8) \quad S_N(v) = \sum_{i=1}^{N-1} -\frac{1}{8}v_i^{2/3} + \frac{1}{6}(\Delta_i v)^2.$$

The advantage of this representation is that S_N is a *strictly convex* function of v (since $t^{2/3}$ is strictly concave for $t \geq 0$).

To prove that a minimizer exists, we need only show that $S_N \rightarrow \infty$ as $\|v\| \rightarrow \infty$. Since the discrete Dirichlet Laplacian is invertible we have $\frac{1}{6} \sum (\Delta_i v)^2 \geq C_1 \|v\|^2$ with $C_1 > 0$. Since $\frac{1}{8} \sum v_i^{2/3} \leq C_2 \|v\|^{2/3}$ we have

$$S_N(v) \geq C_1 \|v\|^2 - C_2 \|v\|^{2/3}.$$

When $\|v\|$ is large the first term on the right is dominant. Therefore a minimizing sequence must stay bounded, and $S_N(v)$ achieves its minimum subject to $v_i \geq 0$. It follows of course that $SE_N(w)$ achieves its minimum subject to $w_i \geq 0$.

Turning to part (b): the uniqueness of the optimal v is clear from the strict convexity of S_N ; we henceforth denote it by v^* . Evidently $\phi_i = (v_i^*)^{1/3}$ is the unique minimizer of $SE_N(w)$ subject to $w_i \geq 0$. Note that $v^* \neq 0$, since the minimum value of S_N is clearly negative (indeed, S_N is negative when v is sufficiently small and nonzero). The positivity of v^* follows immediately from the concavity of its piecewise linear graph, so we turn now to that assertion. By the “piecewise linear graph” associated with a vector $v = (v_1, \dots, v_{N-1})$ we mean the graph of the piecewise linear function taking the value v_i at each $h = i/N$, and value 0 at the endpoints $h = 0$ and $h = 1$. We argue by contradiction: suppose the piecewise linear graph of v^* is not concave, and consider its concave hull. It is the piecewise linear graph of a nonnegative vector \tilde{v} . One easily verifies that $\Delta_i \tilde{v} \leq \Delta_i v^*$ for each i (see Figure 5 and its caption for a brief explanation). But $\tilde{v}_i \geq v_i^*$, with strict inequality for at least one i if the graph of v^* is not concave. Therefore the value of S_N at \tilde{v} is strictly smaller than the value at v^* , contradicting the fact that v^* achieves the minimum. Thus the graph of v^* is concave.

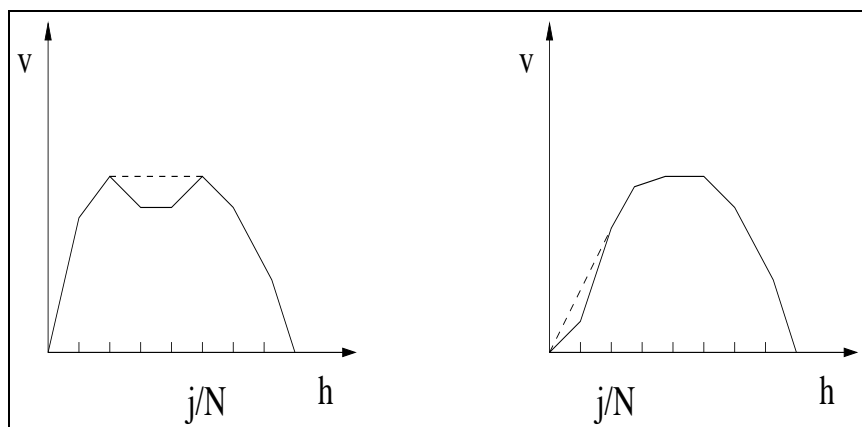


FIGURE 5. Solid line: the piecewise linear graph of v . Dotted line: the piecewise linear graph of \tilde{v} where it differs from that of v . At an interior endpoint of the dotted line (e.g. at $h = j/N$ in either figure), the graph of \tilde{v} has a smaller angle than that of v , so $|\Delta_j \tilde{v}| < |\Delta_j v|$.

Turning now to part (c): we defined v^* by minimizing S_N subject to the constraint $v_i \geq 0$. But we have just shown that each v_i^* is positive, so the constraint does not bind. Therefore v^* is a critical point of S_N , and ϕ (defined by $\phi_i = (v_i^*)^{1/3}$) is a critical point of SE_N . If SE_N had another positive critical point $\bar{\phi}$, then $\bar{v}_i = (\bar{\phi}_i)^3$ would be a positive critical point of S_N . Strict convexity assures us that $\bar{v} = v^*$, whence $\bar{\phi} = \phi$. Thus ϕ is the unique positive critical point of SE_N . \square

In part (c) of Theorem 3.1, the hypothesis of positivity is crucial. Since $SE_N(w) = SE_N(-w)$, $-\phi$ also minimizes SE_N . Moreover, we can get additional critical points by “odd reflection.” For example, suppose $N = 2M$ and let ϕ^M be the unique positive minimizer of SE_M . Then

$$w_i = \begin{cases} \phi_i & \text{for } i = 1, \dots, M-1 \\ 0 & \text{for } i = M \\ -\phi_{2M-i} & \text{for } i = M+1, \dots, 2M-1 \end{cases}$$

is easily seen to be a critical point with N steps. (Since $w_M = \Delta_M w = 0$, the fact that ϕ^M is a critical point for SE_M implies that the first variation of SE_N with respect to w_i vanishes for $i \neq M$. The first variation with respect to w_M also vanishes, since it equals $-\frac{1}{4}w_M + w_M^2 \Delta_M \Delta w^3$ and $w_M = 0$.)

3.3. Existence, uniqueness, and properties of the continuum self-similar solution. The PDE evolution in similarity variables (3.5) is the L^2 steepest-descent associated with

$$(3.9) \quad SE(w) = \int_0^1 -\frac{1}{8}w^2 + \frac{1}{6}[(w^3)_{hh}]^2 dh$$

subject to $w(0) = w(1) = 0$, by a calculation parallel to (2.13). As a consequence, a continuum similarity solution is simply a critical point of this functional. (We shall sometimes write $(w^3)_{hh}^2$ rather than $[(w^3)_{hh}]^2$ for efficiency of notation.)

The methods we used in the discrete setting carry over straightforwardly to the continuum. However, the self-similar solution is not very smooth near the endpoints $h = 0, 1$. Moreover the character of the singularity will be important in what follows. Therefore we must do some extra work to characterize the behavior near the endpoints.

Theorem 3.2. *Consider the “similarity energy” SE defined by (3.9), viewed as a functional on*

$$(3.10) \quad \left\{ w : \int_0^1 (w^3)_{hh}^2 dh < \infty \text{ and } w(0) = w(1) = 0 \right\}.$$

- (a) *The minimum subject to $w \geq 0$ is achieved.*
- (b) *The minimizer ϕ is unique, symmetric, and strictly positive (i.e. $\phi(h) > 0$ for $0 < h < 1$). Moreover, it has the property that the graph of ϕ^3 is concave.*
- (c) *The function $v^*(h) = \phi^3(h)$ satisfies $v_{hhhh}^* = \frac{1}{4}(v^*)^{-1/3}$ with $v^*(0) = v^*(1) = 0$ and $v_{hh}^*(0) = v_{hh}^*(1) = 0$. It is smooth away from the endpoints $h = 0, 1$, and it approaches 0 linearly at the endpoints (i.e. $v_h^*(0) = -v_h^*(1)$ exists and is strictly positive).*
- (d) *At the endpoints $v_{hhhh}^* \rightarrow \infty$, but $\int_0^1 |v_{hhhh}^*|^p dy < \infty$ for every $p < 3$. As a consequence, v^* is C^3 and its third derivative is uniformly α -Hölder continuous for any $\alpha < 2/3$.*
- (e) *v^* is the only positive solution of $v_{hhhh} = \frac{1}{4}v^{-1/3}$ with $v(0) = v(1) = 0$, $v_{hh}(0) = v_{hh}(1) = 0$, and the regularity stated in (d).*

Proof. As in the discrete setting, it is convenient to work with $v = w^3$, in terms of which SE equals

$$(3.11) \quad S(v) = \int_0^1 -\frac{1}{8}v^{2/3} + \frac{1}{6}v_{hh}^2 dh,$$

which is strictly convex for $v \geq 0$.

To prove that a minimizer exists, we use the direct method of the calculus of variations. Convexity implies lower semicontinuity, and $\|v_{hh}\|_{L^2}$ is equivalent to the $H^2([0, 1])$ norm when $v(0) = v(1) = 0$, so it suffices to show that $S(v) \rightarrow \infty$ as $\|v_{hh}\|_{L^2} \rightarrow \infty$. By Hölder’s and Poincaré’s inequalities $\int_0^1 v^{2/3} dh \leq (\int_0^1 v^2 dh)^{1/3} \leq C_1(\int_0^1 v_h^2 dh)^{1/3}$. Since $\int_0^1 v_h dh = 0$ we also have $\int_0^1 v_h^2 dh \leq C_2 \int_0^1 v_{hh}^2 dh$. So

$$S(v) \geq \frac{1}{6}\|v_{hh}\|_{L^2}^2 - C\|v_{hh}\|_{L^2}^{2/3}.$$

When $\|v_{hh}\|_{L^2}$ is large the first term on the right is dominant. Therefore a minimizing sequence must stay bounded in H^2 , and $S(v)$ achieves its minimum subject to $v \geq 0$. Since $SE(w) = S(w^3)$, it follows that $SE(w)$ achieves its minimum subject to $w \geq 0$.

As in the discrete setting, the uniqueness of the optimal v is clear from the strict convexity of S ; we henceforth denote it by v^* . Uniqueness implies symmetry: $v^*(h) = v^*(1-h)$ since otherwise $v^*(1-h)$ would be a distinct minimizer of S . Note that v^* is not identically 0, since the minimum value of S is clearly negative. Clearly $\phi = (v^*)^{1/3}$ is the minimizer of $SE(w)$ subject to $w \geq 0$.

The positivity of v^* follows immediately from the concavity of its graph, so we turn now to that assertion. Consider the concave hull of the graph of v^* : it is the graph of a positive function $\tilde{v} \geq v^*$. If $\tilde{v} = v^*$ we are done. Otherwise the graph of \tilde{v} includes a straight segment lying strictly above the graph of v^* , with endpoints on the graph of v^* . We label the endpoints $(h_1, v^*(h_1))$ and $(h_2, v^*(h_2))$, where $0 \leq h_1 < h_2 \leq 1$ (see Figure 6). Suppose $h_1 > 0$ and $h_2 < 1$. Then the segment has slope $v_h^*(h_1) = v_h^*(h_2)$ (indeed, if the segment is the graph of $ah + b$ then $ah + b - v^*(h)$ achieves

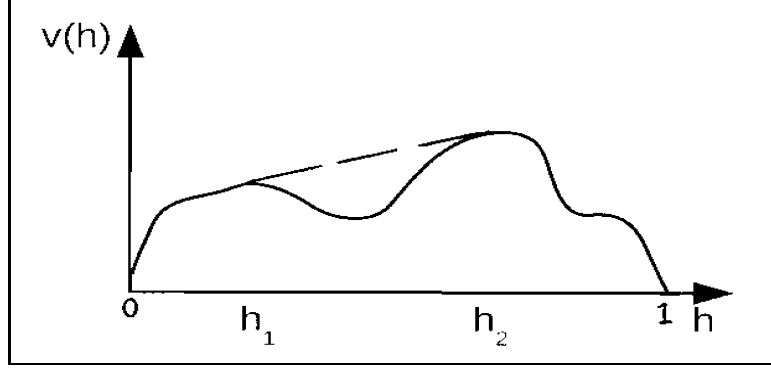


FIGURE 6. If the graph of v^* is not concave then its convex envelope includes a straight segment.

its minimum at h_1 and h_2 ; note that v^* is differentiable since $v_{hh}^* \in L^2$). Now consider the function $\bar{v}(h)$ defined by

$$\text{graph of } \bar{v} = \begin{cases} \text{graph of } v^* & \text{for } h \leq h_1 \text{ and } h \leq h_2 \\ \text{the segment} & \text{for } h_1 \leq h \leq h_2. \end{cases}$$

Evidently $\int_0^1 \bar{v}^{2/3} dh > \int_0^1 (v^*)^{2/3} dh$ and $\int_0^1 \bar{v}_{hh}^2 dh < \int_0^1 (v^*)_{hh}^2 dh$. So the value of S at \bar{v} is strictly below that at v^* , contradicting the hypothesis that v^* achieved the minimum. If $h_1 = 0$ or $h_2 = 0$ the argument is almost the same: when h_i is an endpoint, we no longer know that the slope of the segment matches $v_h^*(h_i)$, but we no longer need this either. (The matching condition was used only to know that $\bar{v}_{hh} \in L^2$.)

We turn now to parts (c) and (d), whose proofs will be intertwined. The PDE $v_{hhhh}^* = \frac{1}{4}(v^*)^{-1/3}$ is the Euler-Lagrange equation of S . (To avoid boundary terms when integrating by parts, it suffices to take the first variation with respect to compactly supported test functions.) Since v^* is strictly positive away from the endpoints, the right hand side is a smooth function of v^* ; it follows easily that v^* is smooth away from the endpoints. In considering what happens near the endpoints, we need only consider $h = 0$, by symmetry. Since the graph of v^* is concave, we have an estimate of the form

$$(3.12) \quad v^*(h) \geq Ch \quad \text{for } h \text{ near } 0$$

with $C > 0$. (Indeed, between $h = 0$ and $h = 1/2$ the graph lies above the line joining the origin to $(1/2, v^*(1/2))$, so we may take $C = 2v^*(1/2)$). Therefore $|v_{hhhh}^*| \leq C'h^{-1/3}$ near $h = 0$, and $|v_{hhhh}^*|^p$ is integrable for $p < 3$. Using the inequality

$$|f(h_2) - f(h_1)| \leq \left(\int_{h_1}^{h_2} |f_h|^p dh \right)^{1/p} |h_2 - h_1|^{(p-1)/p}$$

we conclude that v_{hh}^* is uniformly α -Hölder continuous for any $\alpha < 2/3$. In particular, $v_h^*(0)$ exists – and it must be positive, by (3.12). The remaining assertion of parts (c) and (d) is that $v_{hh}^*(0) = v_{hh}^*(1) = 0$. This comes, of course, by taking the first variation of $S(v)$ and paying attention to the boundary terms. If \dot{v} is a smooth function of h that vanishes at $h = 0$ and $h = 1$,

the vanishing of the first variation requires that

$$\begin{aligned}
 0 &= \int_0^1 -\frac{1}{12}(v^*)^{-1/3}\dot{v} + \frac{1}{3}v_{hh}^*\dot{v}_{hh} dh \\
 (3.13) \quad &= \int_0^1 \int \frac{1}{3} \left[-\frac{1}{4}(v^*)^{-1/3} + v_{hhhh}^* \right] \dot{v} dh + \frac{1}{3}v_{hh}^*\dot{v}_h|_0^1 - \frac{1}{3}v_{hhh}^*\dot{v}|_0^1 \\
 &= \frac{1}{3}v_{hh}^*\dot{v}_h|_0^1
 \end{aligned}$$

using the PDE and the boundary condition on \dot{v} for the last line. Since $\dot{v}_h(0)$ and $\dot{v}_h(1)$ are unrestricted, we conclude that $v_{hh}^*(0) = v_{hh}^*(1) = 0$.

Part (e) is standard: we have just proved that the PDE (with the stated boundary conditions and regularity hypothesis) amounts to the vanishing of the first variation of S . This implies uniqueness, since S is strictly convex. \square

We note that while $v^* = \phi^3$ is C^3 , the function ϕ is much more singular: indeed, its first derivative $\phi_h = \frac{1}{3}(v^*)^{-2/3}v_h^*$ blows up like a constant times $h^{-2/3}$ as $h \rightarrow 0$.

We discussed in Section 2.4 the conjecture that in the continuum setting, the region occupied by steps should “have finite extent.” In the continuum setting, our $u(h, t)$ is the slope as a function of height and time. It determines the height as a function of space and time, $h(x, t)$, by integration. The distance between the leading step and the trailing step is evidently

$$(3.14) \quad x|_{h=1} - x|_{h=0} = \int_0^1 x_h dh = \int_0^1 \frac{1}{u} dh.$$

So the steps have finite extent exactly if $1/u$ is integrable. Since $h^{-2/3}$ is integrable, the similarity solution has this property:

Proposition 3.3. *The continuum similarity solution $u(h, t) = (1 + t)^{-1/4}\phi(h)$ has the property that the steps have finite extent. In fact, they occupy an interval whose length is proportional to $(1 + t)^{1/4}$.*

4. THE DISCRETE SOLUTION IS ASYMPTOTICALLY SELF-SIMILAR

This section proves that in the discrete setting (i.e. with N held fixed) the slope evolution is asymptotically self-similar. The logic of the argument is simple: the rescaled slope w evolves by l^2 -steepest descent of SE_N , and this function has a unique positive critical point. So we expect w to converge to the critical point as time tends to infinity.

There is however a catch: the uniqueness result requires strict positivity. So we need to know that each w_i stays bounded away from 0. Fortunately, this is true:

Lemma 4.1. *Let $w = (w_1(s), \dots, w_{N-1}(s))$ solve the discrete evolution in similarity variables, (3.2), with positive initial data. Define*

$$z(s) = \|\Delta^{-1}(1/w)\|^2$$

where $1/w$ is the vector $(w_1^{-1}, \dots, w_{N-1}^{-1})$, Δ^{-1} is the matrix that inverts the discrete Dirichlet Laplacian (2.16), and we use the l^2 norm on \mathbb{R}^{N-1} . Then z satisfies

$$(4.1) \quad \frac{dz}{ds} \leq -\frac{1}{4}z + Cz^{1/2}$$

where C depends only on the initial data. As a consequence, z stays uniformly bounded and each w_i stays bounded away from 0.

Proof. Differentiating with respect to s gives

$$\frac{1}{2} \frac{dz}{ds} = \langle \Delta^{-1}(1/w), \Delta^{-1}(1/w)_s \rangle.$$

Now, the evolution law for w can be written as

$$(1/w)_s = -\frac{1}{4}(1/w) + \Delta(\Delta w^3).$$

So we have

$$\begin{aligned} \frac{1}{2} \frac{dz}{ds} &= \langle \Delta^{-1}(1/w), -\frac{1}{4}\Delta^{-1}(1/w) + \Delta^{-1}\Delta\Delta w^3 \rangle \\ &= -\frac{1}{4}z + \langle \Delta^{-1}(1/w), \Delta w^3 \rangle \\ &\leq -\frac{1}{4}z + z^{1/2}\|\Delta w^3\| \end{aligned}$$

To prove (4.1), we need to show that $\|\Delta w^3\|$ stays uniformly bounded. From the definition (3.7) of SE_N , we have

$$\|\Delta w^3\|^2 = 6SE_N(w) + \frac{3}{4}\|w\|^2$$

Now, the evolution is steepest descent for SE_N , so this functional is monotonically decreasing. Moreover the L^2 norm also decreases, by an argument similar to the proof of Lemma 2.2:

$$\begin{aligned} \frac{1}{2} \frac{d}{ds} \|w\|^2 &= \langle w, w_s \rangle \\ &= \langle w, -\frac{1}{4}w - \partial_{t^2} E_N(w) \rangle \\ &= -\frac{1}{4}\|w\|^2 - 6E_N(w) \leq 0. \end{aligned}$$

(Here E_N is the functional defined by (2.11), and we used (2.15) in the last step.) Thus $\|\Delta w^3\|^2$ is bounded by the initial value of $6SE_N(w) + \frac{3}{4}\|w\|^2$, and (4.1) is proved.

The remaining assertions of the Lemma are elementary: since the right side of (4.1) is negative for $z > (4C)^2$, z is bounded for all $s > 0$ by $\max\{z(0), (4C)^2\}$. Since we are in the discrete setting, multiplication by Δ is a bounded operator, and $\|1/w\| = \|\Delta\Delta^{-1}(1/w)\| \leq C'z^{1/2}$. Thus $1/w_i$ is bounded for each $i = 1, \dots, N-1$, uniformly in s . So w_i remains bounded away from 0. \square

With this result in hand, the proof of asymptotic self-similarity is easy. Note that the following result is global in character: *every* solution is asymptotically self-similar, regardless of its initial data (provided the initial slopes are positive, i.e. the initial step profile is monotone).

Theorem 4.2. *Let $w = (w_1(s), \dots, w_{N-1}(s))$ solve the discrete evolution in similarity variables, (3.2), with positive initial data. Then w is asymptotically self-similar, in the sense that $w(s) \rightarrow \phi$ as $s \rightarrow \infty$, where ϕ is the similarity solution (the unique positive solution of (3.3)).*

Proof. The evolution of w is steepest-descent for $SE_N(w)$. Since SE_N is bounded below and control of SE_N implies a bound on $\|w\|$, $w(s)$ stays uniformly bounded as $s \rightarrow \infty$. We conclude, by a standard result from ODE theory, that the ω -limit set of $w(s)$ consists of critical points of SE_N . Moreover by Lemma 4.1 w stays uniformly positive, so only *positive* critical points can occur. By Theorem 3.1 there is only one such critical point, our self-similar solution ϕ . Since the ω -limit set contains only ϕ , $w(s)$ converges to ϕ as $s \rightarrow \infty$. \square

5. CONVERGENCE OF THE SELF-SIMILAR SOLUTIONS AS $N \rightarrow \infty$

The continuum self-similar solution $\phi(h)$ minimizes the continuum self-similar energy (3.9), while the discrete self-similar solution (let us call it ϕ^N , to emphasize the dependence on N) minimizes the finite-difference analogue of that functional, (3.7). Therefore it is natural to expect that $\phi^N \rightarrow \phi$ as $N \rightarrow \infty$. This is indeed the case, as we prove in the present section. (The result would be routine if ϕ were smooth. But ϕ is singular at the endpoints; our essential task is therefore to assess the impact of its singular behavior).

As usual in discussing the convergence of a numerical approximation scheme, we must either (a) estimate the difference between the discrete solution $\phi^N = (\phi_1^N, \dots, \phi_{N-1}^N)$ and the nodal values of $\phi(h)$, or (b) estimate the difference, in a suitable function space, between ϕ and an interpolant of ϕ^N . We choose the latter approach.

Since our problem involves second derivatives, the convenient interpolation operator associates a discrete function with a piecewise quadratic one. To define it, let $\Delta h = 1/N$, let $h_i = i/N$ be our usual equispaced gridpoints, and let $h_{i+\frac{1}{2}} = (i + \frac{1}{2}) \Delta h$ be the midpoints of the intervals they determine. Then for any discrete function η with nodal value η_i at h_i and $\eta_0 = \eta_N = 0$, its interpolant $\tilde{\eta}^N(h)$ is

- (i) linear on $[0, h_{\frac{1}{2}}]$ and $[h_{N-\frac{1}{2}}, 1]$, matching the discrete function at the endpoints of these intervals; and
- (ii) quadratic on each interval $[h_{j-\frac{1}{2}}, h_{j+\frac{1}{2}}]$, $j = 1, \dots, N-1$, with values and derivatives at the endpoints that match those of the discrete function in the sense that

$$(5.1) \quad \begin{aligned} \tilde{\eta}^N \left(h_{j-\frac{1}{2}} \right) &= \frac{\eta_j + \eta_{j-1}}{2}, & \tilde{\eta}^N \left(h_{j+\frac{1}{2}} \right) &= \frac{\eta_j + \eta_{j+1}}{2} \\ \tilde{\eta}_h^N \left(h_{j-\frac{1}{2}} \right) &= \frac{\eta_j - \eta_{j-1}}{\Delta h}, & \tilde{\eta}_h^N \left(h_{j+\frac{1}{2}} \right) &= \frac{\eta_{j+1} - \eta_j}{\Delta h}. \end{aligned}$$

Condition (ii) might seem at first overdetermined, since a quadratic polynomial has just three parameters. It is not, since the specified data meet the consistency condition

$$\tilde{\eta}^N \left(h_{j-\frac{1}{2}} \right) - \tilde{\eta}^N \left(h_{j+\frac{1}{2}} \right) = \frac{\Delta h}{2} \left[\tilde{\eta}_h^N \left(h_{j-\frac{1}{2}} \right) + \tilde{\eta}_h^N \left(h_{j+\frac{1}{2}} \right) \right].$$

The interpolant $\tilde{\eta}^N(h)$ is uniquely determined by (5.1); it vanishes at the endpoints $h = 0, 1$ and belongs to $H^2(0, 1)$; moreover

$$(5.2) \quad \int_0^1 (\tilde{\eta}^N)_{hh}^2 dh = \frac{1}{N} \sum_{i=1}^{N-1} (\Delta_i \eta)^2$$

since $(\tilde{\eta}^N)_{hh} = \Delta_i \eta$ on $(h_{i-\frac{1}{2}}, h_{i+\frac{1}{2}})$.

Since $SE(w)$ is convex as a function of $v = w^3$, the natural convergence estimate involves ϕ^3 rather than ϕ :

Theorem 5.1. *Let $v_i^N = (\phi_i^N)^3$ be the cube of the discrete self-similar solution, and let \tilde{v}^N be the piecewise-quadratic interpolant defined by (5.1). Then \tilde{v}^N converges to the cube of the continuum self-similar solution in $H^2(0,1)$ with convergence rate $N^{-5/6}$ in the sense that $\int_0^1 (\tilde{v}^N - \phi^3)_{hh}^2 dh \leq CN^{-5/3}$.*

Proof. Since we are discussing the discrete and continuous settings at the same time, it is important to normalize SE_N by $1/N$, so it behaves like an integral as $N \rightarrow \infty$. We therefore define

$$(5.3) \quad \overline{SE}_N(w) = \frac{1}{N} SE_N(w) = \frac{1}{N} \sum_{i=1}^{N-1} -\frac{1}{8} w_i^2 + \frac{1}{6} (\Delta_i w^3)^2$$

(defined as always using the convention that $w_0 = w_N = 0$).

Our argument has three main steps. Taken together, Steps 1 and 2 demonstrate that SE and \overline{SE}_N have approximately the same minimum value. Then Step 3 uses a convexity argument complete the proof.

Step 1: $\min \overline{SE}_N \leq \min SE + CN^{-5/3}$. Indeed, let ϕ be the continuous self-similar solution, and consider the trial function $w_i = \phi(i/N)$ in the definition of \overline{SE}_N . We claim that

$$(5.4) \quad \left| \int_0^1 \phi^2 dh - \frac{1}{N} \sum_{i=1}^{N-1} \phi^2(h_i) \right| \leq CN^{-5/3}$$

and

$$(5.5) \quad \left| \int_0^1 (\phi^3)_{hh}^2 dh - \frac{1}{N} \sum_{i=1}^{N-1} (\Delta_i \phi^3)^2 \right| \leq CN^{-2}.$$

The assertion of Step 1 follows immediately from these relations.

We shall make repeated use of the estimate

$$(5.6) \quad \left| \int_{h_i}^{h_{i+1}} f dh - \frac{f(h_i) + f(h_{i+1})}{2} \Delta h \right| \leq C (\Delta h)^2 \int_{h_i}^{h_{i+1}} |f_{hh}| dh,$$

which follows easily from the fact that if $g(0) = g(1) = 0$ then $|\int_0^1 g dh| \leq C \int_0^1 |g_{hh}| dh$.

Preparing to address (5.4), we recall from Theorem 3.2 that $v = \phi^3$ is smooth, symmetric, and uniformly positive away from the endpoints $h = 0, 1$; moreover v is (uniformly) $C^{3,\alpha}$, and $v_h(0)$ is strictly positive. Since

$$(\phi^2)_{hh} = (v^{2/3})_{hh} = -\frac{2}{9} v^{-4/3} v_h^2 + \frac{2}{3} v^{-1/3} v_{hh},$$

we have

$$|(\phi^2)_{hh}| \leq C \max\{h^{-4/3}, (1-h)^{-4/3}\}$$

for $0 < h < 1$. Applying (5.6) on (h_i, h_{i+1}) for $i = 1, \dots, N-2$, adding, and using that $\sum_{i=1}^{N-1} \max\{h_i^{-4/3}, (1-h_i)^{-4/3}\} \leq CN^{4/3}$, we conclude that

$$\left| \int_{h_1}^{h_{N-1}} \phi^2 dh - \frac{1}{N} \sum_{i=1}^{N-2} \frac{\phi^2(h_i) + \phi^2(h_{i+1})}{2} \right| \leq CN^{-5/3}.$$

The left hand side equals

$$\left| \int_{h_1}^{h_{N-1}} \phi^2 dh - \frac{1}{N} \left(\frac{\phi^2(h_1)}{2} + \phi^2(h_2) + \dots + \phi^2(h_{N-2}) + \frac{\phi^2(h_{N-1})}{2} \right) \right|,$$

which differs from the left hand side of (5.4) by

$$\int_0^{h_1} \phi^2 dh + \int_{h_{N-1}}^1 \phi^2 dh + \frac{1}{2N} \phi^2(h_1) + \frac{1}{2N} \phi^2(h_{N-1}).$$

Since $\phi^2(h) = v^{2/3}(h) \leq Ch^{2/3}$ near $h = 0$, the first and third terms are at most $CN^{-5/3}$. By symmetry, the same estimate applies to the other two terms. Thus (5.4) holds.

Turning now to (5.5), we continue to work with $v = \phi^3$. We have

$$|(v_{hh})_{hh}^2| = |2v_{hh}^2 + 2v_{hh}v_{hhhh}| \leq C \max\{h^{-1/3}, (1-h)^{-1/3}\},$$

using the PDE $v_{hhhh} = \frac{1}{4}v^{-1/3}$ along with the linear behavior of v near $h = 0, 1$. Applying (5.6) on (h_i, h_{i+1}) for $i = 0, \dots, N-1$, adding, and noting that $h^{-1/3}$ is integrable at 0, we conclude that

$$(5.7) \quad \left| \int_0^1 v_{hh}^2 dh - \frac{1}{N} \sum_{i=1}^{N-1} v_{hh}^2(h_i) \right| \leq CN^{-2} \int_0^1 |(v_{hh})_{hh}^2| dh \leq CN^{-2}.$$

Now consider the difference between $\Delta_i v = N^2[v(h_{i-1}) - 2v(h_i) + v(h_{i+1})]$ and $v_{hh}(h_i)$: by Taylor expansion,

$$|v_{hh}(h_i) - \Delta_i v| \leq CN^{-2} \max_{h_{i-1} \leq h \leq h_{i+1}} |v_{hhhh}| \leq CN^{-2} \max\{h_{i-1}^{-1/3}, (1-h_{i+1})^{-1/3}\}$$

for $i = 2, \dots, N-2$. Since v_{hh} is uniformly bounded, so is $\Delta_i v$ (uniformly for $i = 2, \dots, N-2$), whence

$$|v_{hh}^2(h_i) - (\Delta_i v)^2| \leq C |v_{hh}(h_i) - \Delta_i v| \leq CN^{-2} \max\{h_{i-1}^{-1/3}, (1-h_{i+1})^{-1/3}\}.$$

Adding, we conclude that

$$\left| \frac{1}{N} \sum_{i=2}^{N-2} v_{hh}^2(h_i) - \frac{1}{N} \sum_{i=2}^{N-2} (\Delta_i v)^2 \right| \leq CN^{-3} \sum_{i=2}^{N-2} \max\{h_{i-1}^{-1/3}, (1-h_{i+1})^{-1/3}\}.$$

The right hand side is of order N^{-2} . The left hand side lacks terms associated with $i = 1$ and $i = N-1$, however

$$|v_{hh}(h_1)| \leq CN^{-1}$$

since v_{hh} is uniformly C^1 and $v_{hh}(0) = 0$; also

$$|\Delta_1 v| \leq CN^{-1}$$

since $v(h) = v_h(0)h + O(h^3)$ near zero, using Taylor expansion, $v(0) = v_{hh}(0) = 0$, and the uniform boundedness of v_{hhh} . The situation near $h = 1$ is symmetric. Thus the terms associated with the extreme values of i are negligible, and we have shown that

$$(5.8) \quad \left| \frac{1}{N} \sum_{i=1}^{N-1} v_{hh}^2(h_i) - \frac{1}{N} \sum_{i=1}^{N-1} (\Delta_i v)^2 \right| \leq CN^{-2}.$$

The estimate (5.5) follows immediately from (5.7) and (5.8). This completes Step 1.

Step 2: $\min SE \leq \min \overline{SE}_N + CN^{-5/3}$. Indeed, let $v_i = \phi_i^3$ where ϕ is the discrete self-similar solution, and consider its piecewise quadratic interpolant \tilde{v}^N . We have

$$\int_0^1 (\tilde{v}^N)_{hh}^2 dh = \frac{1}{N} \sum_{i=1}^{N-1} (\Delta_i v)^2$$

by (5.2), and one easily verifies that

$$\left| \int_0^1 (\tilde{v}^N)^{2/3} dh - \frac{1}{N} \sum_{i=1}^{N-1} (\tilde{v}^N)^{2/3}(h_i) \right| \leq CN^{-5/3}$$

by arguing as for (5.4). Taken together, these give the assertion of Step 2.

Step 3: $\int_0^1 (\tilde{v}^N - \phi^3)_{hh}^2 dh \leq CN^{-5/3}$. Remember that $SE(w) = S(w^3)$, where

$$(5.9) \quad S(\eta) = \int_0^1 -\frac{1}{8}\eta^{2/3} + \frac{1}{6}\eta_{hh}^2 dh$$

is strictly convex. Taken together, Steps 1 and 2 show that

$$(5.10) \quad S(\tilde{v}^N) - S(v) \leq CN^{-5/3}$$

where $v = \phi^3$ and \tilde{v}^N is the piecewise-quadratic interpolant of ϕ_i^3 . By second-order Taylor expansion of the quadratic function $\frac{1}{2}|\xi|^2$ (which is exact since the function is quadratic) we have

$$(5.11) \quad \frac{1}{2}|\tilde{v}_{hh}^N|^2 - \frac{1}{2}|v_{hh}|^2 = v_{hh}(\tilde{v}_{hh}^N - v_{hh}) + \frac{1}{2}|\tilde{v}_{hh}^N - v_{hh}|^2.$$

By the convexity of $-v^{2/3}$ we have

$$(5.12) \quad -\frac{1}{8}(\tilde{v}^N)^{2/3} + \frac{1}{8}v^{2/3} \geq -\frac{1}{12}v^{-1/3}(\tilde{v}^N - v).$$

Multiplying (5.11) by $\frac{1}{3}$, integrating (5.11) and (5.12) over $[0, 1]$, then adding the resulting expressions, we get

$$S(\tilde{v}^N) - S(v) \geq \int_0^1 \frac{1}{3}v_{hh}(\tilde{v}_{hh}^N - v_{hh}) - \frac{1}{12}v^{-1/3}(\tilde{v}^N - v) + \frac{1}{6}|\tilde{v}_{hh}^N - v_{hh}|^2 dh.$$

Integrating the first term on the right hand side by parts and using that $v = v_{hh} = 0$ at the boundary, we get

$$S(\tilde{v}^N) - S(v) \geq \int_0^1 \left(\frac{1}{3}v_{hhhh} - \frac{1}{12}v^{-1/3} \right) (\tilde{v}^N - v) + \frac{1}{6}|\tilde{v}_{hh}^N - v_{hh}|^2 dh.$$

But $v_{hhhh} - \frac{1}{4}v^{-1/3} = 0$, so the first term vanishes and we have

$$S(\tilde{v}^N) - S(v) \geq \int_0^1 \frac{1}{6} |\tilde{v}_{hh}^N - v_{hh}|^2 dh.$$

Combining this with (5.10), we conclude that

$$\int_0^1 |\tilde{v}_{hh}^N - v_{hh}|^2 dh \leq CN^{-5/3},$$

confirming the assertion of Step 3 and completing the proof of the theorem. \square

6. DISCUSSION

We have discussed the evolution of a monotone step train separating two facets in the attachment-detachment-limited regime. By focusing on the slope as a function of height we have achieved a rather complete understanding of the discrete problem; in particular we have shown that the solution exists for all time and is asymptotically self-similar.

Our understanding of the continuous problem is much less complete: we have not proved asymptotic self-similarity, nor have we even discussed the existence or uniqueness of solutions to (2.9). However we have identified a similarity solution in the continuous setting, by minimizing SE . Moreover we have explored its properties in detail. In addition, we have shown uniqueness assuming positivity and some regularity, and we have shown that it is the continuum limit of our discrete self-similar solutions.

Can similar methods be used to address the continuous time-dependent problem? We hope so, but this will apparently require additional ideas. In both Sections 2 and 4, the positivity of the discrete solution (u_i in Section 2, w_i in Section 4) was used in a crucial way. We do not know even a “formal proof” of positivity in the time-dependent continuous setting. (The proof of Lemma 4.1 has a continuous analogue, if w is regular enough to support the necessary integrations by parts. However this gives only that $\Delta^{-1}(1/w) \in L^2$, where $\Delta^{-1}(1/w) = f$ is the solution of $f_{hh} = 1/w$ with $f(0) = f(1) = 0$. Such an estimate permits w to vanish at isolated points. The same remark applies also to the solution of the slope PDE (2.9): if it is regular enough to support the necessary integrations by parts, then we can argue as for Lemma 2.4 to get $\Delta^{-1}(1/u) \in L^2$. However this would not prevent u from vanishing at isolated points.)

What about *local stability* of the continuous self-similar solution, for the evolution in similarity variables? We certainly expect it to be true. Linearized stability – more specifically, strict positivity of the Hessian of SE , viewed as a function of $v = w^3$ – is elementary. (It was this strict convexity that drove the proof of Theorem 5.1.)

Self-similar behavior is also seen numerically for the analogous problem with diffusion-limited step dynamics [6]. Can our approach be used in that setting? Unfortunately, we don’t see how. Our analysis relies heavily on the steepest-descent structure of the slope evolution law. In the diffusion-limited setting the discrete slope evolution law is $\dot{y}_i = -y_i^2 \Delta_i[y \Delta y^3]$ and the analogue of (2.9) is $u_t = -u^2[u(u^3)_{hh}]_{hh}$. These evolutions seem not to have a steepest-descent character analogous to that of the attachment-detachment-limited version.

We have concentrated on the slope as a function of height. The key advantage of this viewpoint is that there is no free boundary: h always ranges from 0 to 1. This viewpoint is however limited

to the study of monotone step trains in one space dimension. For a profile with peaks and valleys we expect steps to collide, so the maximum and minimum height would change with time.

APPENDIX A. PHYSICAL BASIS OF THE STEP ODES

This Appendix reviews the derivation of the step equations (2.1) and the meaning of the attachment-detachment-limited regime. This material is well-known; similar discussions can be found, for example, in [6, 10, 11, 17].

Consider a monotone one-dimensional step train as shown in Figure 1, and let $c_i(x, t)$ be the concentration of adatoms on the terrace between x_i and x_{i+1} . Ignoring evaporation and deposition, c_i solves the diffusion equation

$$\frac{\partial c_i}{\partial t} = D_s \Delta c_i$$

where D_s is the terrace diffusion constant. Working in the quasistatic approximation, we replace this by

$$(A.1) \quad \Delta c_i = 0 \quad \text{for } x_i < x < x_{i+1}$$

with $\Delta c_i = (c_i)_{xx}$ since the model is one-dimensional.

The boundary conditions for (A.1) links the adatom flux $J_i = -D_s(c_i)_x$ to the equilibrium adatom densities at the steps, through “sticking coefficients” k_u and k_d (which may be different, due to the Ehrlich-Schwoebel effect):

$$(A.2) \quad \begin{aligned} -J_i(x_i, t) &= k_d(c_i(x_i, t) - c_i^{eq}) \\ J_i(x_{i+1}, t) &= k_u(c_i(x_{i+1}, t) - c_{i+1}^{eq}), \end{aligned}$$

where c_i^{eq} is the equilibrium adatom concentration on the i th step (to be specified presently). Thinking three-dimensionally (i.e. viewing each step as a line and each terrace as a strip), c_i represents atoms per unit area while J_i represents atoms per unit length per unit time, so k_u and k_d have dimensions length/time.

The advantage of the quasistatic approximation is that we can easily solve (A.1)-(A.2) exactly. Indeed: $(c_i)_{xx} = 0$ implies $c_i(x, t) = a_i(t)x + b_i(t)$, and the boundary conditions lead easily to

$$(A.3) \quad a_i = \frac{c_{i+1}^{eq} - c_i^{eq}}{(x_{i+1} - x_i) + D_s \left(\frac{1}{k_u} + \frac{1}{k_d} \right)}.$$

Now the step velocity is determined by conservation of mass: the i th step advances at a rate proportional to the net flux of atoms into it (or recedes, if the flux is negative):

$$(A.4) \quad \begin{aligned} \frac{dx_i}{dt} &= \Omega(J_i - J_{i-1}) \\ &= \Omega D_s (a_i - a_{i-1}) \\ &= \Omega D_s \left[\frac{c_{i+1}^{eq} - c_i^{eq}}{(x_{i+1} - x_i) + D_s \left(\frac{1}{k_u} + \frac{1}{k_d} \right)} - \frac{c_i^{eq} - c_{i-1}^{eq}}{(x_i - x_{i-1}) + D_s \left(\frac{1}{k_u} + \frac{1}{k_d} \right)} \right] \end{aligned}$$

where Ω (the area occupied by a single atom) has dimension (length)².

To complete the model we must specify the equilibrium concentration c_i^{eq} at the i th step, which enters the boundary condition (A.2). Linearizing the relation

$$c_i^{eq} = c^{eq} \exp \frac{\mu_i}{k_B T}$$

where c^{eq} is the equilibrium concentration at an isolated step, k_B is the Boltzmann constant, T is temperature, and μ_i is the chemical potential of the i th step, we take

$$(A.5) \quad c_i^{eq} = c^{eq} \left(1 + \frac{\mu_i}{k_B T} \right).$$

It remains to discuss the chemical potential μ_i , which is (by definition) the amount by which the free energy changes when the step moves one atomic distance. Since (for a monotone step train) steps are neither created nor annihilated, we can ignore the self-energy of the steps. The free energy \mathcal{E} is therefore entirely due to step interaction:

$$(A.6) \quad \mathcal{E} = \sum_i f \left(\frac{x_{i+1} - x_i}{\alpha} \right)$$

where α is the height of each step (the atomic distance) and the functional form of f reflects the physics of step interaction. We follow convention in focusing on entropic interaction, which leads to the choice

$$(A.7) \quad f(t) = c_0 t^{-2}$$

where c_0 has the dimensions of energy. Combining the definition

$$\mu_i = -\alpha \frac{\partial \mathcal{E}}{\partial x_i}$$

with our choice of \mathcal{E} gives

$$(A.8) \quad \mu_i = c_0 f' \left(\frac{x_{i+1} - x_i}{\alpha} \right) - c_0 f' \left(\frac{x_i - x_{i-1}}{\alpha} \right) = -\frac{2c_0 \alpha^3}{(x_{i+1} - x_i)^3} + \frac{2c_0 \alpha^3}{(x_i - x_{i-1})^3}.$$

The model is now fully specified. Taking $k_u = k_d = k$ for simplicity, the velocity of the i th step is

$$(A.9) \quad \frac{dx_i}{dt} = \frac{\Omega D_s c^{eq}}{k_B T} \left[\frac{\mu_{i+1} - \mu_i}{(x_{i+1} - x_i) + 2D_s/k} - \frac{\mu_i - \mu_{i-1}}{(x_i - x_{i-1}) + 2D_s/k} \right]$$

with μ_i given by (A.8).

The attachment-detachment-limited (ADL) version of the step dynamics is obtained by making a further approximation. The denominator of each term in (A.9) depends on the relative sizes of the terrace width $l_i = x_{i+1} - x_i$ and the attachment length D_s/k . When $D_s/k \gg l_i$, diffusion across the terraces is fast and the dynamics is limited by the attachment and detachment processes (this is the ADL regime). In the opposite case, when $D_s/k \ll l_i$, the dynamics is limited by diffusion across the terraces (this is the diffusion-limited or DL regime). The expression for the step velocity

simplifies in these cases, becoming

$$(A.10) \quad \frac{dx_i}{dt} = \frac{\Omega k c^{eq}}{2k_B T} (\mu_{i+1} - 2\mu_i + \mu_{i-1}) \quad \text{in the ADL regime, and}$$

$$(A.11) \quad \frac{dx_i}{dt} = \frac{\Omega D_s c^{eq}}{k_B T} \left(\frac{\mu_{i+1} - \mu_i}{x_{i+1} - x_i} - \frac{\mu_i - \mu_{i-1}}{x_i - x_{i-1}} \right) \quad \text{in the DL regime.}$$

In this paper we have focused on the ADL regime. Our starting point (2.1) was therefore a non-dimensionalized version of (A.10). The equations for the extreme steps are obtained similarly, with the convention that the adatom concentration vanishes identically on the facets (to the right of x_N and to the left of x_1), so that the extreme steps experience a flux of adatoms only from one side.

APPENDIX B. CONSISTENCY WITH THE CONVENTIONAL HEIGHT PDE

This Appendix checks the formal consistency of our slope PDE with the more conventional approach to surface evolution, based on a PDE for the surface height as a function of position and time. There is evidence in the radial setting that DL step dynamics is inconsistent with a widely-used PDE for $h(x, t)$ [13]; the discussion here shows that there is no such inconsistency in our one-dimensional, monotone, ADL setting.

The “more conventional approach” we have in mind describes the evolution of a continuous, monotone profile $h(x, t)$ such that $h = 0$ for $x < x_L(t)$ and $h = 1$ for $x > x_R(t)$. The PDE is

$$(B.1) \quad h_t + j_x = 0$$

where the “surface current” j is

$$j = \begin{cases} -m(h_x)\mu_x & \text{for } x_L < x < x_R \\ 0 & \text{otherwise} \end{cases}$$

Here $\mu = -\frac{3}{2}(h_x^2)_x$ is the first variation of $\int \frac{1}{2}h_x^3 dx$ and $m(h_x)$ is a suitable mobility. In general the mobility is a constant times $(1 + \frac{2D_s}{\alpha k}|h_x|)^{-1}$; in the ADL setting this reduces after nondimensionalization to

$$m(h_x) = \frac{1}{|h_x|}$$

and the PDE becomes

$$(B.2) \quad h_t = -\frac{3}{2} \left(\frac{1}{h_x} (h_x^2)_{xx} \right)_x \quad \text{for } x_L(t) < x < x_R(t).$$

It is not difficult to see that this PDE is the continuum version of our step equations, by repeated use of the principle that the continuum version of $f(x_{i+1}) - f(x_i)$ is $f_x \frac{\alpha}{h_x}$ where α is the step height.

Equation (B.2) is quite singular near x_L and x_R since we expect h_x to approach zero there. Moreover x_L and x_R are free boundaries, whose evolution is at best determined implicitly. Therefore the existence and uniqueness of solutions is open. But we now check that a (sufficiently regular) solution of (B.2) determines a solution of our slope PDE (2.9).

We start by differentiating (B.2) with respect to x , to get an equation for the slope as a function of space and time, $F(x, t) = h_x(x, t)$: clearly

$$(B.3) \quad F_t = -\frac{3}{2} \left(\frac{1}{F} (F^2)_{xx} \right)_{xx}.$$

Now suppose $u(h, t)$ is defined not by the slope PDE, but rather by the relation $F(x, t) = u(h(x, t), t)$. Then $F_t = u_t + u_h h_t = u_t - \frac{3}{2}u_h (F^{-1}(F^2)_{xx})_x$. Using chain rule in the form $g_x = g_h h_x = g_h u$ we have

$$\frac{3}{2} (F^{-1}(F^2)_{xx})_x = \frac{3}{2} u (u^{-1} u (u(u^2)_h)_h)_h = u(u^3)_{hhh}.$$

Taking another x derivative, we get

$$\frac{3}{2} (F^{-1}(F^2)_{xx})_{xx} = u(u(u^3)_{hhh})_h = u^2(u^3)_{hhhh} + uu_h(u^3)_{hhh}$$

Thus (B.3) is equivalent to

$$u_t - u_h u(u^3)_{hhh} = -u^2(u^3)_{hhhh} - uu_h(u^3)_{hhh}$$

which simplifies to our slope PDE $u_t = -u^2(u^3)_{hhhh}$.

What about boundary conditions? The continuity equation (B.1) should hold weakly across $x = x_L$ and $x = x_R$. Since h should be continuous there, this requires that j be continuous, in other words (B.1) includes the implicit requirement that $\frac{1}{h_x}(h_x)_{xx}^2$ approach 0 as $x \downarrow x_L$ and as $x \uparrow x_R$. This is equivalent to our condition for the slope PDE that $(u^3)_{hh} = 0$ at $h = 0, 1$, since the relation $F(x, t) = u(h(x, t), t)$ implies

$$(u^3)_{hh} = \frac{1}{F} \left(\frac{1}{F} (F^3)_x \right)_x = \frac{3}{2} \frac{1}{F} (F^2)_{xx}$$

and the edges of the facets correspond to $h = 0, 1$.

A key advantage of working with the slope as a function of height is that the task of finding the facet edge is decoupled from the PDE. Rather than solve a free boundary problem, we have only to solve the slope PDE for $u(h, t)$, then integrate to find the inverse of the height function using the relation $x(h, t) - x_L(t) = \int_0^h u^{-1} dh$. Taking $h = 1$, we get $x_R(t) - x_L(t) = \int_0^1 u^{-1} dh$. If due to symmetry we expect $x_R(t) = -x_L(t)$ (this is the case, for example, for our self-similar solution) then $x_R(t) = -x_L(t) = \frac{1}{2} \int_0^1 u^{-1} dh$. Thus $x(h, t)$ is fully determined, and so is its inverse function $h(x, t)$. Without symmetry, we need an extra relation to determine the ‘‘constant of integration’’ $x_L(t)$. This relation is $\int_0^1 x(h) dh = \text{constant}$ (the continuum version of $\sum_{i=1}^N \dot{x}_i = 0$, which follows immediately from the step equations (2.1)-(2.4)).

REFERENCES

1. A. J. Bernoff and T. P. Witelski, *Stability and dynamics of self-similarity in evolution equations*, J. Eng. Math. **DOI 10.1007** (2009), s10665-009-9309-8.
2. W. K. Burton, N. Cabrera, and F.C. Frank, *The growth of crystals and the equilibrium structure of their surfaces*, Philos. Trans. R. Soc. London **Ser. A 243** (1951), 299-358.
3. W. E and N. K. Yip, *Continuum theory of epitaxial growth. i*, J. Stat. Phys. **104** (2001), 221-253.
4. J. Eggers and M. A. Fontelos, *The role of self-similarity in singularities of partial differential equations*, Nonlinearity **22** (2008), R1-R44.
5. P. W. Fok, R. R. Rosales, and D. Margetis, *Unification of step bunching phenomena on vicinal surfaces*, Phys. Rev. B **76** (2007), 033408.
6. ———, *Facet evolution on supported nanostructures: the effect of finite height*, Phys. Rev. B **78** (2008), 235401.
7. N. Israeli, H. C. Jeong, D. Kandel, and J. D. Weeks, *Dynamics and scaling of one-dimensional surface structures*, Phys. Rev. B **61** (2000), 5698-5706.
8. N. Israeli and D. Kandel, *Profile scaling in decay of nanostructures*, Phys. Rev. Lett. **80** (1998), 3300-3303.
9. ———, *Profile of a decaying crystalline cone*, Phys. Rev. B **62** (1999), 5946-5962.

10. ———, *Decay of one-dimensional surface modulations*, Phys. Rev. B **62** (2000), 13707–13717.
11. H. C. Jeong and E. D. Williams, *Steps on surfaces: experiment and theory*, Surf. Sci. Rep. **34** (1999), 171–294.
12. D. Margetis, M. J. Aziz, and H. A. Stone, *Continuum approach to self-similarity and scaling in morphological relaxation of a crystal with a facet*, Phys. Rev. B **71** (2005), 165432.
13. D. Margetis, P. W. Fok, M. J. Aziz, and H. A. Stone, *Continuum theory of nanostructure decay via a microscale condition*, Phys. Rev. Lett. **97** (2006), 096102.
14. D. Margetis and R. V. Kohn, *Continuum relaxation of interacting steps on crystal surfaces in 2 + 1 dimensions*, Multisc. Model. Simul. **5** (2006), 729–758.
15. D. Margetis and K. Nakamura, *From crystal steps to continuum laws: Behavior near large facets in one dimension*, Preprint (2010).
16. P. Nozieres, *On the motion of steps on a vicinal surface*, J. Phys. I (France) **48** (1987), 1605–1608.
17. M. Ozdemir and A. Zangwill, *Morphological equilibration of a corrugated crystalline surface*, Phys. Rev. B **42** (1990), 5013–5024.
18. A. Pimpinelli and J. Villain, *Physics of crystal growth*, Cambridge University Press, 1998.
19. A. Rettori and J. Villain, *Flattening of grooves on a crystal surface: A method of investigation of surface roughness*, J. Phys. I (France) **49** (1988), 257–267.
20. V. Shenoy and L. B. Freund, *A continuum description of the energetics and evolution of stepped surfaces in strained nanostructures*, J. Mech. Phys. Solids **50** (2002), 1817–1841.
21. V. B. Shenoy, A. Ramasubramaniam, and L. B. Freund, *A variational approach to nonlinear dynamics of nanoscale surface modulations*, Surf. Sci. **529** (2003), 365–383.
22. V. B. Shenoy, A. Ramasubramaniam, H. Ramanarayan, D. T. Tambe, W-L. Chan, and E. Chason, *Influence of step-edge barriers on the morphological relaxation of nanoscale ripples on crystal surfaces*, Phys. Rev. Lett. **92** (2004), 256101.
23. H. Spohn, *Surface dynamics below the roughening transition*, J. Phys. I France **3** (1993), 69–81.
24. L.-H. Tang, *Flattening of grooves: from step dynamics to continuum theory*, Dynamics of Crystal Surfaces and Interfaces (P. M. Duxbury and T. J. Pence, eds.), Plenum Press, New York, NY, 1997, pp. 169–184.
25. Y. Xiang, *Derivation of a continuum model for epitaxial growth with elasticity on a vicinal surface*, SIAM J. Appl. Math. **63** (2002), 241–258.
26. Y. Xiang and W. E, *Nonlinear evolution equation of the stress-driven morphological instability*, J. Appl. Phys. **91** (2002), 9414–9422.

COURANT INSTITUTE, NYU, NEW YORK, NY 10012

E-mail address, Hala Al Hajj Shehadeh: hala@cims.nyu.edu

Current address, Hala Al Hajj Shehadeh: Dept. of Mathematics, University of Michigan, Ann Arbor, MI 48109

E-mail address, Robert Kohn: kohn@cims.nyu.edu

E-mail address, Jonathan Weare: weare@cims.nyu.edu

Current address, Jonathan Weare: Department of Mathematics, University of Chicago, Chicago, IL 60637